Macromolecules

ARTICLE

pubs.acs.org/Macromolecules

Single Chain Asymmetric Block Copolymers in Poor Solvents. Candidates for Patchy Colloids

Ryan M. Holmes* and David R. M. Williams

Department of Applied Mathematics, Research School of Physical Sciences and Engineering, Australian National University, Canberra, Australia

Supporting Information

ABSTRACT: Single chain block copolymers in poor solvents with asymmetric **A** and **B** species block lengths form an interesting and potentially useful set of conformations not yet fully investigated by the literature. Self-consistent field theory simulations performed in this work predict that the chains collapse to form a sphere of the species with longer blocks surrounded by various surface domains of the species with shorter blocks. A simple free energy scaling model describes this formation and provides an alternative prediction of the *number* of such surface domains formed for a large range of polymer parameters. The model and simulation predictions of the number of surface domains agree well for the majority of cases, and best for highly asymmetric polymer chains. The authors believe that these highly asymmetric polymer chains are candidates for building patchy colloid like particles, as they form balls with a controllable number of surface patches.

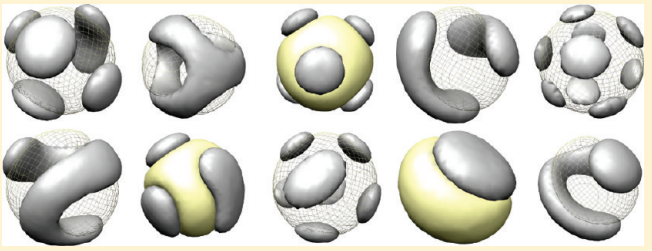

INTRODUCTION

Block copolymers have received much attention due to their tendency to self-assemble into intricately structured nanoscale particles and networks. The chemically distinct blocks forming the polymer chain repel each other out of energetic considerations but cannot entirely separate due to chain connectivity, resulting in microphase separation. An enormous variety of interesting conformations and structures form depending on polymer architecture, interaction strengths, solvent conditions and other parameters. The understanding of these conformations and the reasons for their formation is vital to a range of applications from protein folding[1] and drug delivery[2] to materials science and nanoscience.[3]

Most block copolymer studies focus on high density polymer solutions without an explicit solvent due to their applications in materials science. For these copolymer melts, the agreement between theory and experiment is now quite good and their conformations can be predicted accurately.[4] This is not true for some classes of single copolymer chains in dilute solutions. There exist many studies on so-called $H-P$ copolymers in dilute solutions, consisting of a mix of hydrophobic (H) monomers and hydrophilic polar (P) monomers. $H-P$ copolymer globules are characterized by the formation of a densely packed H core surrounded by a P fringe layer, due to the solvent selectivity. These polymers are of interest due to their similarity to proteins and their properties, such as the coil−globule transition, have been studied extensively.[5−7] This paper focuses on copolymers where the solvent is *nonselectively poor for both species* and therefore each individual chain collapses to form its own densely packed and intricately structured globule, with sharp interfaces between components. Apart from the homopolymer case,[8] a full understanding of the conformations formed by these single chain copolymers in nonselective poor solvents has not yet been reached. Studies done using Monte Carlo and self-consistent field theory simulations have shown the range of interesting and potentially useful conformations that flexible single chain block copolymers in nonselective poor solvents can form.[9,10] These studies focused on copolymers with symmetric block lengths of two monomer species. This paper aims to investigate the asymmetric case, where the length of the blocks of the two species are different.

We focus our attention on fully flexible single chain asymmetric block copolymers with repeating blocks of **A** and **B** species monomers where the **A** blocks contain less monomers than the **B** blocks. We consider only nonselective poor solvents, meaning the chains collapse into a compact globule with no preference between **A** and **B** species to solvent contact. We will show that this class of polymer may have the potential to be used as patchy colloid like particles[11−13] in nanoscience applications due to the conformation into which they collapse.

We use a self-consistent field theory (SCFT) simulation method to obtain predictions of the collapsed polymer conformations. SCFT is significantly faster than other methods such as Monte Carlo, allowing a much broader and more thorough investigation of the parameter space. SCFT has been used extensively for the study of polymer melts.[14,15]

Received: January 13, 2011
Revised: May 19, 2011
Published: July 13, 2011

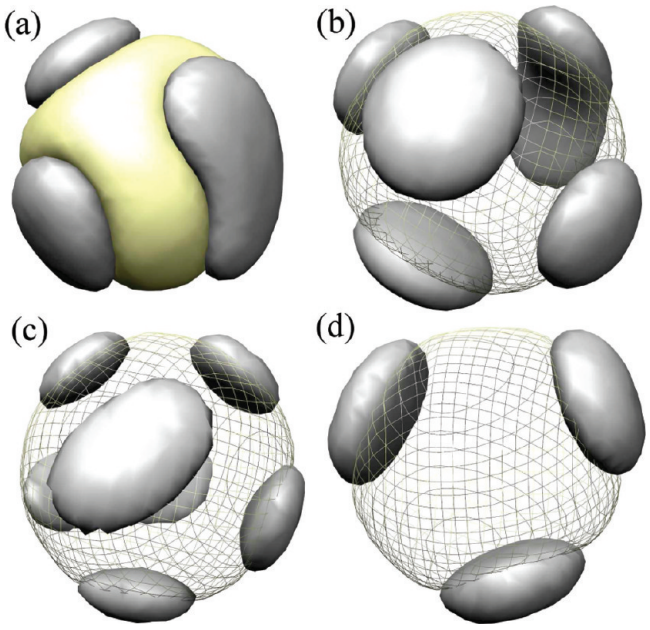

Figure 1. Polymer conformations produced using SCFT for various polymer chain parameters.[17] The polymer chains have N total monomers, n blocks and block size ratio $\mathscr{R} = N_A/N_B$ where N_A and N_B are the number of species **A** and **B** monomers. The flory interaction parameters polymer−solvent and polymer−polymer are χ and χ_{AB} respectively. For the above conformations: (a): $N = 6000$, $n = 16$, $\mathscr{R} = 0.55$, $\chi = 0.65$, $\chi_{AB} = 0.25$. (b): $N = 8192$, $n = 16$, $\mathscr{R} = 0.45$, $\chi = 0.65$, $\chi_{AB} = 0.25$. (c): $N = 9284$, $n = 22$, $\mathscr{R} = 0.25$, $\chi = 0.7$, $\chi_{AB} = 0.2$. (d): $N = 5520$, $n = 12$, $\mathscr{R} = 0.3$, $\chi = 0.7$, $\chi_{AB} = 0.3$.

The SCFT simulations predict that the chains collapse to form a sphere of the species with longer blocks surrounded by various surface domains of the species with shorter blocks (see Figure 1). On the basis of this result, we construct a free energy scaling model of the polymer system using simple surface tension and stretching free energy terms. This model gives a simple theoretical prediction of the conformation formed given the various polymer parameters and solvent strength. Specifically, using this model we are able to accurately predict the number of surface **A** domains formed for highly asymmetric single block copolymer chains in poor solvents. This conformation of a spherical globule with a predictable and hence controllable number of surface patches would be ideal for use as a patchy colloid like particle.[16]

We first describe the theoretical basis and numerical implementation of the self-consistent field theory simulation method for single polymer chains. The free energy scaling model is described and analyzed in the following section. The results and analysis section presents the main results of the simulations and compares them to the free energy model. Finally, we conclude and summarize the outcomes of this research and suggest further work to be done.

SCFT SIMULATION METHOD

Theoretical Basis. Self-consistent field theory is based on a density field model of the polymer.[4] The polymer is described by density fields on a lattice that are iteratively updated using a propagator function q that reproduces the boltzmann distribution in the arrangement of the polymer chain. This propagator function returns the connected polymeric nature to the density fields.

We consider a polymer chain with N monomers and monomer size (Kuhn length) b. The chain consists of n alternating blocks of species **A** and species **B** monomers. The block size ratio $\mathscr{R}$ determines the degree of asymmetry in the polymer chain, with $\mathscr{R} = N_A/N_B$ where N_A is the total number of **A** monomers and N_B the total number of **B** monomers. Dividing the chain into T_s steps (for computation T_s is usually not equal to N), the partition function from the beginning of the chain given that the chain begins at $\mathbf{r}_0$ is denoted $Q(\mathbf{r},\mathbf{r}_0,s)$. We are placing no restrictions on the beginning and ending positions of the chain, and so we work with the partition function integrated over all starting positions, the *forward propagator* $q(\mathbf{r},s) = \int_V Q(\mathbf{r},\mathbf{r}_0,s)\ \mathrm{d}\mathbf{r}_0$. The forward propagator obeys a modified diffusion equation:[18,19]

$$\frac{\partial}{\partial s} q(\mathbf{r},s) = \frac{b^2}{6}\nabla^2 q(\mathbf{r},s) - w(\mathbf{r},s)q(\mathbf{r},s) \qquad (1)$$

Here $w(\mathbf{r},s)$ is the mean potential felt by the sth segment in the mean field approximation. The initial condition is $q(\mathbf{r},0) = 1$, as the chain can start anywhere.

There is a corresponding *backward propagator* $q^\dagger(\mathbf{r},s)$, being the integrated partition function beginning at the end of the chain (again at any point) and reaching the point $\mathbf{r}$ in $T_s - s$ steps. This satisfies a similar diffusion equation with the initial condition $q^\dagger(\mathbf{r},T_s) = 1$. The total partition function can be constructed from the forward and backward propagators:

$$Z = \int_V q(\mathbf{r},s)q^\dagger(\mathbf{r},s)\ \mathrm{d}\mathbf{r} = \int_V q(\mathbf{r},T_s)\ \mathrm{d}\mathbf{r}$$

Here the second equality is true because the integral is independent of the step s allowing us to use the initial condition on $q^\dagger$. Given this partition function, the polymer density contribution ϕ_s of each step along the chain is obtained from:

$$\phi_s = \left(\frac{T_s}{N}v\right)\frac{q(\mathbf{r},s)q^\dagger(\mathbf{r},s)}{Z} \qquad (2)$$

Here $v = {}^4/_3\pi b^3$ is the monomer volume. From this the total densities ϕ_A of species **A** monomers and ϕ_B of species **B** monomers can be obtained by summing over all step density contributions to the appropriate species.

The free energy of a particular polymer conformation contains several contributions. The polymer configurational entropy portion of the free energy comes from the partition function Z above. The other contributions are (units of k_BT are adopted throughout):

Polymer−solvent interaction energy, described by the Flory interaction parameter χ:[20]

$$F_{PS}|_{\text{site}} = \chi(\phi_A + \phi_B)(1 - \phi_A - \phi_B)$$

Polymer−polymer interaction energy, described by the interaction parameter χ_{AB}:

$$F_{AB}|_{\text{site}} = \chi_{AB}\phi_A\phi_B$$

Translational entropy of the solvent given by[8]

$$F_S|_{\text{site}} = (1 - \phi_A - \phi_B)\ log(1 - \phi_A - \phi_B)$$

The mean field $w(\mathbf{r},s)$ can be obtained by minimizing these free energy terms with respect to the polymer densities ϕ_A and ϕ_B. Carrying out this minimization, if s is in an **A** portion of the chain then

$$\begin{aligned} w(\mathbf{r},s) &= w_A(\mathbf{r}) \\ &= \chi(1 - 2\phi_A - 2\phi_B) + \chi_{AB}\phi_B - log(1 - \phi_A - \phi_B) \end{aligned}$$

Similarly for s in a **B** portion of the chain:

$$w(r,s) = w_B(r) = \chi(1-2\phi_A-2\phi_B)+\chi_{AB}\phi_A - log(1-\phi_A-\phi_B)$$

These mean field formulas are used in the diffusion equation (eq 1) to evaluate the propagators.

Numerical Implementation. The SCFT simulation process involves iteratively performing the following steps:

1 Start with random initial density fields ϕ_A and ϕ_B
2 Calculate the mean potentials w_A and w_B generated by these density fields
3 Calculate the forward and backward propagators along the polymer chain given the mean potentials using the *propagator equation* (eq 1)
4 Find new density fields using (eq 2)
5 Use these new density fields in step 2

We use a 3*D* lattice box of size 51 × 51 × 51 units. The polymer densities ϕ_A and ϕ_B are initialized as random normalized fields within a sphere of radius two-thirds of the half lattice box side length (25), centered in the lattice box. We choose the monomer size b such that the total polymer volume (vN) is an 80th of the box volume as this was found to be optimal for minimizing finite lattice size effects and allowing efficient computation.

The most computationally difficult step is solving the propagator equation (step 3). We use an approximate analytic solution to this equation in terms of an integral (see Supporting Information: Appendix 2 for derivation[10]):

$$q(r,s+\delta s) = \gamma\, exp\left(\delta s \frac{b^2}{6}\nabla^2\right) q(r,s)$$

with $\gamma = \exp(-\delta s\, \exp(b^2\delta s/12\nabla^2)w(r))$. The exponential is calculated through:

$$exp\left(\delta s\frac{b^2}{6}\nabla^2\right) q(r,s) = \left(\frac{3}{2\pi\delta s b^2}\right)^{3/2} \int exp\left(-\frac{3|r-r'|^2}{2b^2\delta s}\right) q(r',s)\, dr' \quad (3)$$

Similarly, it is calculated for the exponential in the coefficient γ with $\delta s \rightarrow \delta s/2$ and $q(r',s) \rightarrow w(r)$

The integral (eq 3) above is computationally time-consuming to solve due to the sum over the entire lattice for each lattice point. We use a randomized integration method to speed up the calculation. Clearly because of the exponential, only points $\mathbf{r}'$ within a certain distance R_{max} of $\mathbf{r}$ provide a significant contribution to the integral. For each integer radius within R_{max}, two random points are chosen and appropriately averaged to approximate the entire integral contribution at this radius. Hence for each radius less than R_{max}, only 2 points are added rather than $\propto R^2$, significantly boosting the speed of the calculation. The propagators are renormalized after each integration to prevent large values developing.

The forward and backward propagators q and $q^\dagger$ are functions of position and monomer step along the chain. We use 500 total steps along the chain. The number of monomers per step, or step size ds, is not constant along the chain. We use a smaller step size inside the smaller **A** blocks as this is required to converge to a solution efficiently.

With most SCFT simulations, the entire propagator is solved in one go, and then the entire density field is updated. It was found that for single chains, the simulation was more stable if after each propagator step along the chain, the corresponding portion of the density field was updated immediately. The process involves solving the propagator for step s (using the value from step $s-1$) and step $T_s - s$ (using the value from step $T_s - s + 1$) by performing the integral (eq 3). The density contributions ϕ_s and ϕ_{Ts-s} and the full densities ϕ_A and ϕ_B are then updated. The mean fields w_A and w_B are recalculated and the next steps $s+1$ and $T_s - s - 1$ are solved. The updating of the density contribution ϕ_s involves using both the forward and backward propagator at this step. In some cases one of these must be taken from the previous iteration, since it has not yet been calculated for the current iteration. This somewhat slowed the evolution of the density fields, but was advantageous as it improved the stability of the simulation.

The simulations were only stable for a limited range of the parameter space. We used several additional methods to improve the stability. These included a stabilizing term in the mean potential proportional to the change in the mean potential from the previous step. This term opposed rapid changes in the mean potential slowing the evolution and preventing large gradients from developing. This improved the stability significantly but was small enough to have negligible effect on the conformation (with a maximum over the lattice of less than 1% of all other mean field terms at equilibrium[21]).

We included a free energy calculation in the calculation to provide a quantitative measure of the stability of any given run. For stable runs the free energy plots simply described an almost monotonic decrease to the final equilibrium state. Any deviation from this trend indicated instabilities. The free energy calculation was also used to eliminate semistable conformations and differentiate between different conformations arising from the same initial polymer parameters.

For most polymer configurational parameters, 25 iterations were sufficient to reach a stable polymer conformation. This stability was checked by running some simulations for 40 or more iterations.[21] Depending on the polymer configurational parameters, there was no significant change in the conformation after around 20 iterations. We judged conformations that were not stable (not sufficiently collapsed) after 20 iterations as invalid.

Figure 1 shows some initial valid conformations produced by the simulations for asymmetric copolymers. Clearly the general conformation formed is that of the smaller species **A** (gray) surrounding the larger species **B** (yellow/mesh). The reason for this general trend is explained using the theoretical model in the next section. Species **A** forms a different number of surface domains depending on the polymer chain characteristics. In the next section, we focus on a theoretical prediction of the number of surface domains formed.

LENS FREE ENERGY MODEL

In this section we develop a simple free energy model to describe the polymer system. We consider two factors that contribute to the free energy of a particular block copolymer system; *surface tension* interaction energies between the different components (**A**, **B** and solvent) and entropic *chain stretching*. In a poor solvent, the interaction between the polymer and solvent causes the polymer to collapse into a compact globule with some density ϕ. For a sufficiently poor solvent, this interaction dominates and the globule formed is approximately spherical. This is reflected in the simulation results (Figure 1). Making the

assumption that the globule is spherical allows us to ignore the polymer−solvent interaction and consider only the polymer−polymer surface tension and the chain stretching terms in making a free energy scaling model.

As this is a poor solvent problem and the polymer is collapsed in a dense globule, it could be expected that the contribution of entropic chain stretching is negligible. However, even in collapsed globules, the chain can still be *locally stretched*. This occurs around the interior **A**−**B** interfaces in the globules considered here. The junction points between the **A** and **B** blocks lie on these interior interfaces, and similar to polymer brushes, there is an effective grafting density of chain segments on the interface. If this grafting density is high, then the chains must *stretch* away from the interface as they would run into each other if they were to move sideways. This stretching is only significant near the interface, but it can result in an entropy loss and significant stretching free energy contribution that favors the formation of more interior **A**−**B** interface, countering the surface tension. The overall collapse of the globule also means that there should be a significant free energy contribution from entropic *chain compression*. This is not considered as it would overly complicate an otherwise simple model that appears to work well without it. The chain compression contribution is mostly constant for a given overall globule size and varies only slightly with respect to the number of surface domains. Its variation would favor the formation of fewer, larger surface domains and therefore acts in a similar way to the surface tension contribution.

Surface Tension. The polymer globule density ϕ can be calculated by assuming a spherical homopolymer of density ϕ. If ϕ at a particular site on a lattice is equal to 1 then the volume associated with that point is set to be a monomer volume $v = {}^4/_3\pi b^3$. If the polymer contains N monomers and forms a sphere of radius R, then since ϕ is the volume fraction of polymer, by volume conservation:

$$\frac{4}{3}\pi R^3\phi = vN \Rightarrow R^3 = \frac{b^3N}{\phi} \tag{4}$$

Hence the number of lattice sites taken up by the polymer is given by:

$$\text{sites} = \frac{\frac{4}{3}\pi R^3}{v} = \frac{N}{\phi}$$

And the free energy is (from the SCFT section):

$$F = (\chi\phi(1-\phi) + (1-\phi)\,log(1-\phi))\frac{N}{\phi}$$

$$= \chi(1-\phi)N + \left(\frac{1}{\phi} - 1\right) log(1-\phi)N$$

Minimizing with respect to ϕ and making a linear approximation between $\chi = 0.6$ and $\chi = 0.8$ gives the approximate density of polymer within the sphere:

$$\phi = 1.4(\chi - 0.42) \tag{5}$$

We consider highly asymmetric block copolymers, where the block size ratio $\mathcal{R} = N_A/N_B$ is small. The simulations predict that the large species **B** becomes centralized and surrounded by various surface domains of the smaller species **A** as shown in Figure 1. We model this type of conformation as containing k *lens-shaped* surface domains of radius x (Figure 2a). The lenses have the same curvature on either side, so it is easy to calculate volumes and surface areas.

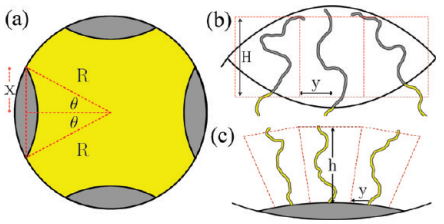

Figure 2. (a) Polymer conformations are modeled as containing k species **A** surface lenses/domains of radius x. (b) Species **A** half blocks simply stretch linearly into cylinders of equal heights in the model. (c) Species **B** half blocks are modeled as stretching into expanding cones.

The **A**−**B** surface tension free energy term can be calculated given the polymer−polymer interaction strength χ_{AB} and the **A**−**B** interaction surface area (see Appendix 1):

$$F_{AB} = \frac{3}{2\sqrt{6}}{\chi_{AB}}^{1/2}k\phi\left(1 - \sqrt{1 - \frac{x^2}{R^2}}\right)\frac{R^2}{b^2} \tag{6}$$

Stretching. The structure of the polymer chain inside a globule is in general very complicated. The exact trajectories followed by the chains can only be obtained by simulation and any analytic model must by its nature be very approximate. For our system, we take a simplified view where each block inside the polymer globule is treated as stretching in its own section of volume—a cone or a cylinder. This simplification of the stretching energy is expected to predict the general trend in the change of the free energy with respect to the various parameters. The exact value of the stretching free energy term is thus only approximate, and we make the assumption that it is accurate up to a premultiplying constant C. Thus, the total free energy is $F_T = F_{AB} + CF_S$, where the parameter C is determined by comparing the model to the results of the SCFT simulations.

The stretching free energy of each species is treated separately. We model the stretching of the larger species **B** as linear stretching into expanding cones (Figure 2c). The cones' base and top are flat, and the base area is set by dividing up the surface area of the lens into equal portions. Each half **B** block is approximated as stretching linearly away from its junction point on the lens surface into the expanding cone shaped volume. This gives a total species **B** stretching free energy of (see Appendix 1):

$$F_{\mathbf{SB}} = \frac{8b^4N_BR^4}{9h\phi^2y^4}(R^{-3} - (R+h)^{-3}) \tag{7}$$

where the height (h) and base radius (y) of the cones are given by:

$$h = R\left(\left(\frac{4b^3N_B}{n\phi y^2R} + 1\right)^{1/3} - 1\right) \tag{8}$$

$$y = R\sqrt{\frac{2k}{n}\left(1 - \sqrt{1 - \frac{x^2}{R^2}}\right)} \tag{9}$$

The chain stretching of species **A** within the lenses is modeled as stretching into cylinders of equal heights (Figure 2b). Since the polymer chain is highly asymmetric, the species **A** stretching is less important than the species **B** stretching. The total species **A**

dx.doi.org/10.1021/ma200085w |*Macromolecules* 2011, 44, 6172–6181

stretching free energy is (see Appendix 1):

$$F_{SA} = \frac{8b^4 N_A}{3\phi^2 y^4} \quad (10)$$

Adding (eq 7) and (eq 10) gives the total stretching free energy F_S of the lens model for a particular lens number k and lens size x. These are related by volume conservation:

$$\frac{N_A}{kN} = 1 - \sqrt{1 - \frac{x^2}{R^2}}\left(1 + \frac{x^2}{2R^2}\right) \quad (11)$$

Minimizing the total free energy $F_T = F_{AB} + CF_S$ with respect to k gives a prediction of the physically expected number of lenses or **A** surface domains. This prediction can be compared to the results of the simulations.

Parameter Trends. The minimum in the total free energy of the lens model arises from the opposite trends of the stretching and the surface tension free energy terms. To minimize surface tension free energy, the system favors a fewer number of lenses k, as this minimizes the total **A**−**B** surface contact area. The stretching free energy term favors more lenses, as the block junction points, located on the **A**−**B** interfaces, have a larger area to spread over.

The opposite trends of the two free energy contributions in the lens model allow simple explanations for the change in the number of surface domains with the various polymer parameters in the real system:

As the polymer−polymer interaction strength χ_{AB} increases, the surface tension free energy term will become more important. The system trends toward less surface domains, as this minimizes **A**−**B** surface contact area.

Polymers with higher total number of blocks n, tend to form more surface domains as the length of each half block is shorter, meaning its stretching becomes more significant. The total number of blocks n also imposes a maximum of $n/2$ on the total number of surface domains that can possibly be formed.

The more highly asymmetric polymers with smaller block size ratios $\mathscr{R}$, form globules with more surface domains. This is because polymers containing less total **A** monomers have less **A**−**B** interface area, making the surface tension term less important. They also have shorter **A** species blocks making the stretching within these blocks more significant.

The trends with the final two parameters, total number of monomers N and polymer−solvent interaction strength χ are less intuitive. They can be investigated by using a series of scaling approximations on the lens model free energy equations. Eliminating constants and parameters that do not depend on χ and N, and noting that:

$$y \propto R, h \propto R, N_A \propto N, N_B \propto N \text{ and } R \propto \left(\frac{N}{\phi}\right)^{1/3}$$

The stretching and surface tension contributions to the free energy become (eqs 6, 7, and 10)):

$$F_{AB} \propto k\phi\left(1 - \sqrt{1 - \frac{x^2}{R^2}}\right)R^2 \approx \phi R^2 \propto N^{2/3}\phi^{1/3}$$

$$F_{SA} + F_{SB} \propto \frac{N}{\phi^2 R^4} + \frac{N}{R\phi^2}(R^{-3} - (R+h)^{-3}) \approx \frac{2N}{\phi^2 R^4} \propto \frac{1}{N^{1/3}\phi^{2/3}}$$

From these relations, it can be seen that as N increases, the surface tension increases and the stretching correspondingly decreases. The number of **A** domains then decreases with increasing N, as the surface tension term begins to dominate.

As χ increases the polymer density ϕ increases (eq 5). The surface tension free energy then increases, because there is a higher density of monomers near the **A**−**B** interaction surface. The number of **A** domains decreases with increasing χ, as the surface tension dominates.

The lens model has provided predictions of how the number of surface domains formed in the collapsed globule depends on each of the five parameters N, n, χ_{AB}, χ, and $\mathscr{R}$. In the Results and Analysis section, the SCFT simulations are shown to reproduce these trends for the majority of cases.

Surface vs Interior Domains. The formation of surface **A** domains and not interior **A** domains can be understood from the free energy terms in the lens model. The parameter C multiplying the stretching free energy terms was set as ≈2 when comparing to the simulations (see next section). Despite this doubling of the value of the stretching terms, the surface tension free energy term was in general larger than the stretching terms at equilibrium. The connected nature of the polymer is therefore less important. The formation of surface domains can be understood as the tendency for a small liquid ball within a significantly larger one to move to the inner surface of the larger ball. The smaller species will form surface domains as this minimizes the species **A**−species **B** surface contact effectively for free, compared to a globule containing interior **A** domains.[21]

RESULTS AND ANALYSIS

Figure 3 and Figure 4 show polymer conformations produced by the SCFT simulations containing a range of different numbers of species **A** surface domains. The figures represents the change in the globule structure while maintaining all parameters constant except the block size ratio $\mathscr{R}$ and the polymer−solvent interaction strength χ respectively. The globule structure trends displayed in these figures reflect the trends predicted by the lens model and shown in the scaling analysis in the Model section.

Figure 5 and Figure 6 show two-dimensional phase diagram slices of the five-dimensional parameter space. The dotted lines separate the diagrams into model predicted regions of constant surface domain number and the SCFT simulation results in the slices are included. Figure 5 shows the globule structure as a function of the total number of monomers N and total block number n. For this slice the agreement between model and simulations is good. It is noteworthy in this phase diagram and in general that the number of surface domains in a given conformation rarely reached the maximum of $n/2$. This is likely because the simulations had difficulty collapsing conformations with a small number of monomers in a particular surface domain. The model prediction indicates that to reach the maximum of $n/2$ surface domains the total number of monomers N must be small (e.g., less than $N = 3000$ to get six domains from an $n = 12$ polymer), so the tendency toward collapse of the overall globule is low and the simulations cannot collapse efficiently in a reasonable number of iterations.

Figure 6 shows the globule structure as a function of χ_{AB} and the block size ratio $\mathscr{R}$. The trend toward more surface domains at lower block size ratios is strong and appears to be modeled well. The SCFT results trend with χ_{AB} appears opposite to that expected from the model at high block size ratios. This could be because of semistable SCFT results, but is most likely because the model is not good in this region of the parameter space. As

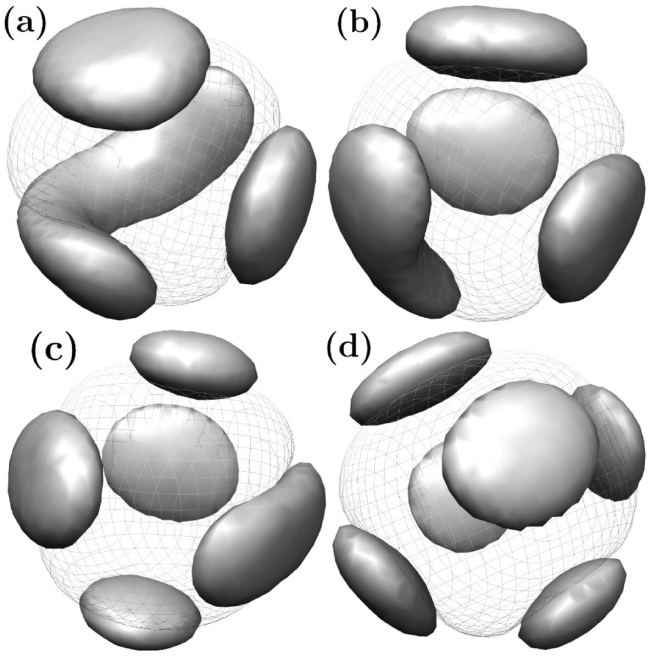

Figure 3. SCFT simulations showing the effect of a decreasing block size ratio $\mathscr{R}$. The parameters $N = 6000$, $n = 16$, $\chi = 0.65$ and $\chi_{AB} = 0.3$ are constant while the block size ratio is (a) $\mathscr{R} = 0.55$, (b) $\mathscr{R} = 0.5$, (c) $\mathscr{R} = 0.4$, and (d) $\mathscr{R} = 0.35$. The number of surface domains k increases as the polymers become more asymmetric, with (a) $k = 3$, (b) $k = 4$, (c) $k = 5$, and (d) $k = 6$. This trend reflects the trend predicted by the lens model, where the number of surface domains would increase because a more asymmetric polymer has less **A**−**B** interface area and the stretching energy becomes more important.

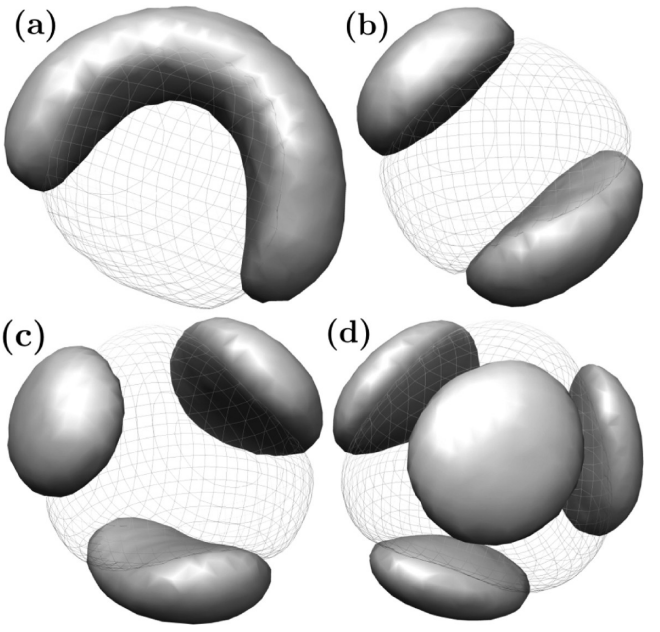

Figure 4. SCFT simulations showing the effect of changing the polymer−solvent interaction strength χ. The parameters $N = 5520$, $n = 12$, $\mathscr{R} = 0.6$, and $\chi_{AB} = 0.25$ are constant while the polymer−solvent interaction strength is (a) $\chi = 0.8$, (b) $\chi = 0.75$, (c) $\chi = 0.65$, and (d) $\chi = 0.6$. The number of surface domains k increases as χ decreases, with (a) $k = 1$, (b) $k = 2$, (c) $k = 3$, and (d) $k = 4$. This trend reflects the trend predicted by the scaling analysis of the lens model equations above, where the number of surface domains would decrease with increasing polymer−solvent interaction strength χ.

discussed below, at high block size ratios long ring conformations appear that are not described well by the lens model.

The simulations done cover a large area of the five-dimensional parameter space and therefore any two-dimensional slice contains only a small number of data points. This is in some part because for a given set of three parameters, the range of the remaining two parameters such that the simulations would converge was often small. This can be seen in Figure 6 where simulations were attempted for a range of χ_{AB} values, but at the low block size ratios, only a couple of χ_{AB} values worked. For these small ranges of parameters, semistable SCFT conformations can have a significant effect on the results as there were only several simulations done in these regions. The study performed was quite general and information on specific regions of phase space is not as thorough as could be obtained with a more focused future study.

Model−Simulation Comparison. Figure 7 plots the number of **A** domains observed in the simulations (simulation value) on the x-axis against the number of **A** domains predicted by the lens model for the same polymer chain configuration. The size of the data point indicates the number of individual simulation results or polymer chain configurations lying on that point.

Clearly the relationship is not one-to-one and there is a large spread in the model predicted values for each simulation value. This spread is most pronounced for the simulation value of 1 **A** domain, where in many cases the model predicts more **A** domains than seen in the simulations. Many of the simulation results do not look like a series of lenses. Instead a range of contorted rings and sausage like shapes are seen, as in Figure 8. The lens model does not describe these kinds of conformations well.

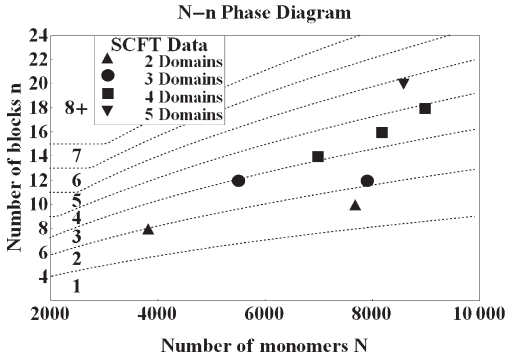

Figure 5. Phase diagram showing the number of surface domains as a function of the number of monomers N and the total block number n (only even n are considered). The parameters $\chi = 0.65$, $\chi_{AB} = 0.15$ and $\mathscr{R} = 0.4$ are constant. The dotted lines split the diagram into model predicted regions of constant surface domain number (indicated inside the n axis). The SCFT simulation points contained in this slice are also included, and in this case the agreement between model and simulations is good.

The majority of conformations containing these elongated domains are formed from relatively symmetric block copolymers with block size ratios greater than $\mathscr{R} \approx 0.45$. An example of this is seen in Figure 6. This suggests that the lens model may describe more asymmetric block copolymers better, because less species **A** monomers results in smaller **A** surface domains and less elongated domains. Eliminating all conformations resulting from polymers with block size ratios greater than $\mathscr{R} = 0.4$ gives the data set shown in Figure 9.

dx.doi.org/10.1021/ma200085w |*Macromolecules* 2011, 44, 6172–6181

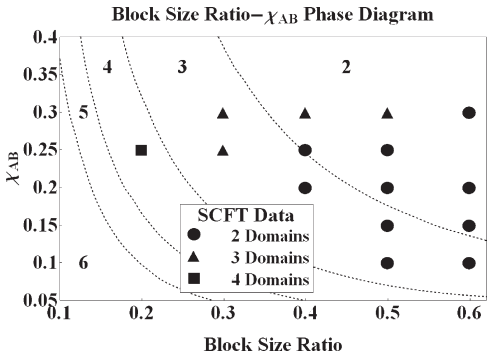

Figure 6. Phase diagram showing the number of surface domains as a function of the polymer−polymer interaction strength χ_{AB} and the block size ratio $\mathscr{R}$. The parameters $N = 5520$, $n = 12$, and $\chi = 0.7$ are constant. The dotted lines split the diagram into regions corresponding to the model predicted regions of constant surface domain number. The SCFT simulation points contained in this slice are also included, and the agreement between model and simulations is good for the lower block size ratios.

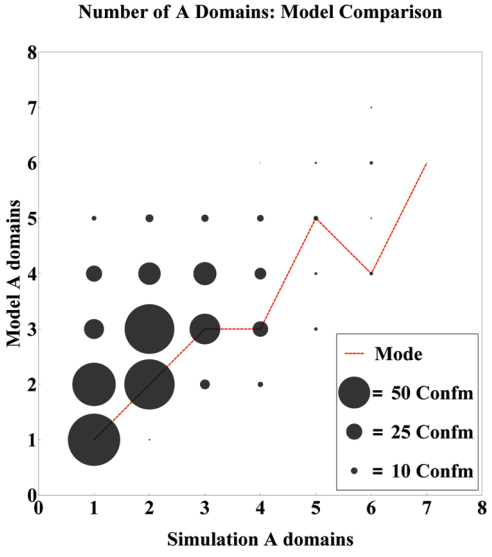

Figure 7. Number of surface **A** domains shown in the simulations versus that predicted by the lens model for the same polymer chain parameters. The size of the data points is proportional to the number of simulations/polymer configurations lying on that point. The line shows the mode at each simulation value. All valid simulation data is included. Fitting constant $C = 2.2$. The large spread is due mainly to conformations containing elongated **A** domains that are not described well by the lens model.

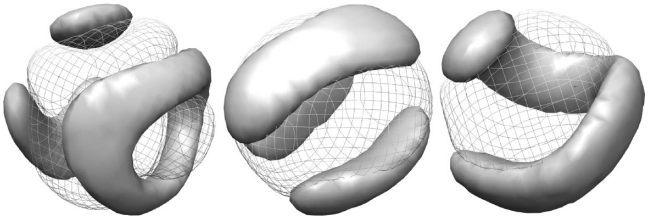

Figure 8. Conformations containing elongated domains not similar to the lens model. Polymer chains forming such conformations are not described well by the lens model.

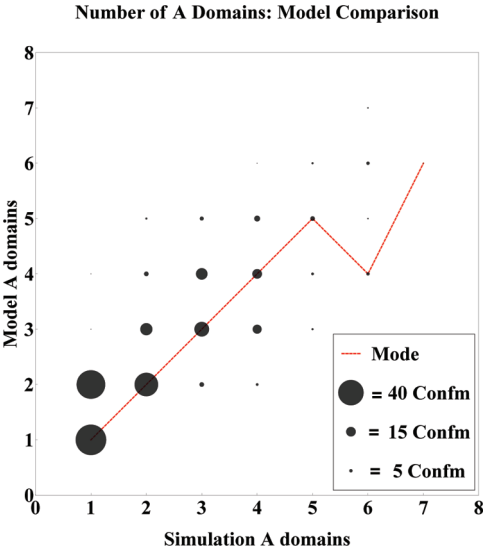

Figure 9. Number of surface **A** domains shown in the simulations versus that predicted by the lens model for the same polymer chain parameters. The size of the data points is proportional to the number of simulations/polymer configurations lying on that point. The line shows the mode at each simulation value. Only conformations resulting from polymer chains with $\mathscr{R} \leq 0.4$ are included. Fitting constant $C = 2.2$. The spread is now less than in Figure 7, especially for the simulation value of 1 **A** domain.

The correspondence between the model and the simulations is now better. In particular, most of the data points with a simulation value of 1 **A** domain and a model prediction of more than 2 **A** domains have been removed. Some outliers from the higher simulation values have also been removed by restricting to highly asymmetric polymer chains. The lens model would split the elongated domains contained in these conformations into two or more sections, resulting in a higher **A** domain number prediction.

The mode of the results now describes a one-to-one relationship for the conformations with smaller numbers of **A** surface domains. The fit is not as good for higher surface domain numbers, possibly because the number of data points here is minimal. This is a good fit considering the simplicity of our model and the complexity of the polymer system. The higher outliers still present in the data, above the mode line, again appear to be due to conformations with elongated domains which are not described well by the lens model. Many of the lower outliers, below the mode line, were found to be unphysical conformations, as discussed in the next section.

Result Validity. Several unphysical conformations, given the polymer chain configuration, were found to be produced by the SCFT simulations. An example is conformation (a) in Figure 10. The polymer chain forming this conformation has a total of six blocks meaning three species **A** blocks. Hence it should not be possible for the conformation to have two species **A** surface domains of equal size. Other examples of unphysical conformations are the 4-equal-ball and 6-equal-ball conformations in Figure 10.

The existence of these unphysical conformations is due to the statistical nature of the SCFT simulations. Abstractly, we can think of the simulation working by propagating every possible polymer chain starting at every possible point through space and giving each possible chain state a weighting according to the

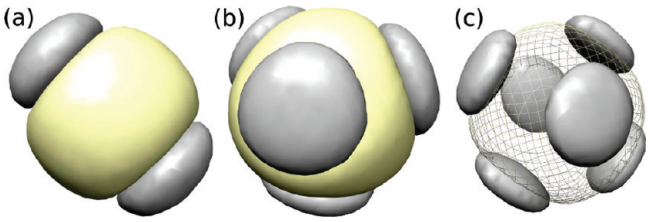

Figure 10. (a) A 3-stack conformation $N = 1890$, $n = 6$, $\mathscr{R} = 0.4$, $\chi = 0.7$, $\chi_{AB} = 0.25$ (surface density =0.15). The two gray **A** species domains have the same size. This should not be possible since there are only 3 **A** blocks. (b) An unphysical 4-equal-ball conformation resulting from a 12 block polymer with only 6 **A** blocks. (c) An unphysical 6-equal-ball conformation resulting from a 18 block polymer with only 9 **A** blocks.

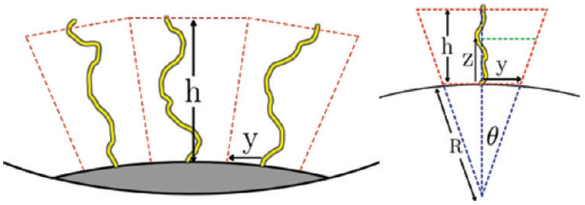

Figure 11. Species **B** stretching model.

mean potential. A chain state that has an **A** block in a **B**-rich density region will be given a small weighting. A polymer chain state with the **A** and **B** blocks in the correct density regions will be given a large weighting. The overall polymer conformation is then obtained by doing a weighted average over all the chain states, given their particular weighting factor. The outputted conformations are therefore averages of many chain arrangements. The 3-stack conformation in Figure 10a could be due to the superposition of polymer chain states having zero, one, two or three blocks in the upper ball. This was confirmed by outputting the density field of each individual **A** block, which were split into disjoint sections covering each surface **A** domain.

This statistical problem where unphysical conformations are produced is fundamental to the SCFT simulation method, and throws the results into some doubt. Eliminating conformations which are found to be unphysical gives a better simulation-model fit, but is not justified as the remaining conformations may suffer from the same problem. This issue may exist in previous work done using SCFT; on polymer melts for example. It may not have been observed before because the location of individual blocks or full polymer chains is unimportant for the overall conformation of a polymer melt. However, this problem may have an effect on the results if, for example, the polymer chains in the melt are not all identical. In this case the location of individual chains is important and as the SCFT method may not correctly locate individual chains, instead creating an overall average, the conformations produced may not be entirely accurate. More research is required to investigate the effects of this problem fully, but clearly more careful checks should be done in the future on the results obtained from SCFT simulations.

Several simulation alterations were tried in an attempt to prevent the formation of these unphysical conformations. An artificial hard sphere term was added to the mean potential surrounding the center of mass of each species **A** block that strongly discouraged any separation of the block into disjoint sections. This was an impractical solution as the radius of the sphere was very difficult to choose correctly to prevent artificial influence on the final conformation. Another alteration attempted was to impose a small artificial repulsion between the different species **A** blocks in the form of an interaction parameter χ_{bl}. Again, this was impractical as the value of χ_{bl} was very difficult to choose correctly to prevent a large artificial influence while still solving the problem.

CONCLUSIONS

We have investigated the properties of single asymmetric block copolymer chains in poor solvents where the blocks of one species (**A**) are significantly shorter than the blocks of the other species (**B**). In general, the self-consistent field theory simulations predicted that the polymer chain collapses into an approximately spherical globule with species **A** forming a number of surface domains surrounding a species **B** core.

We identified a problem due to the statistical aspect of the method where the results produced were sometimes unphysical, given the structure of the polymer chain. This problem is possibly existent in SCFT simulations performed before and may render some results invalid. More research is required to investigate this effect and its impact on SCFT results.

We developed a simple free energy scaling model to explain the simulation results and predict the number of surface **A** domains formed for different chain parameters. The model and simulation predictions of the number of surface domains agreed well for many cases, and best for highly asymmetric polymer chains with $\mathscr{R} \leq 0.4$. The mode of the model-simulation results described an approximate one-to-one relationship. This indicates that our model can predict the conformations formed by highly asymmetric single copolymer chains in nonselective poor solvents reasonably well.

The investigation performed in this work shows the potential of these simple single chain block copolymers to form patchy colloid like particles, due to their tendency to form small **A** domains on the surface of a **B** sphere. The **A** domains constitute the patches on the colloids surface, and their number can be determined from the initial polymer configuration and therefore controlled using the free energy model presented in this paper.

APPENDIX 1: LENS MODEL CALCULATIONS

Surface Tension. The surface area and volume of each lens is found by using the solid angle of the cone $\Omega = 2\pi(1 - \cos\theta)$. The surface area of one side of the lens is given by:

$$A_{(1/2)\mathrm{Lens}} = 4\pi R^2 \frac{\Omega}{4\pi} = 2\pi R^2 \left(1 - \sqrt{1 - \frac{x^2}{R^2}}\right)$$

Substituting into the surface tension free energy equation derived by Helfand and Tagami[22] and multiplying by the number of lenses k gives (eq 6).

Species B Stretching. The free energy resulting from stretching an ideal chain into a cone-shaped volume can be evaluated by generalizing the ideal chain stretching free energy (units of k_bT):[20]

$$F(R) = \frac{3}{2}\frac{R^2}{R_0^2} \qquad (12)$$

The cone is split into discs of infinitesimal height dz and radius $R_c(N)$, each containing dN' monomers where N' is the monomer

number starting at the base of the cone. By conservation of density:

$$\phi\pi[R_c(N')]^2\,\mathrm{d}z = \frac{4}{3}\pi b^3\,\mathrm{d}N' \Longrightarrow \mathrm{d}z = \frac{4b^3\,\mathrm{d}N'}{3\phi[R_c(N')]^2}$$

The ideal stretching equation applies in each infinitesimal disc:

$$\mathrm{d}F_S = \frac{3\mathrm{d}z^2}{2\mathrm{d}N'\,b^2} = \frac{8b^4}{3\phi^2[R_c(N')]^4}\,\mathrm{d}N'$$

Hence integrating over the whole half **B** block of total monomers $N_{(1/2)\mathrm{B}}$:

$$F_{S\mathrm{cone}} = \frac{8b^4}{3\phi^2}\int_0^{N_{(1/2)\mathrm{B}}}[R_c(N')]^{-4}\,\mathrm{d}N' \qquad (13)$$

This gives the stretching free energy penalty for stretching into a cone.

For our **B** species model (Figure 11), the expansion rate of the cone is described by the function $r(z)$ where z is the height above the lens surface along the axis of the cone. The initial radius $r(0) = y$ is set by the requirement that the half lens surface area be taken up by the species **B** stretching cone bases. Given that the polymer has n total blocks, the total junction points is also n and the junction points per lens is n/k. Hence:

$$A_{\mathrm{cone\ base}} = \frac{A_{(1/2)\mathrm{Lens}}}{\mathrm{junction\ points}} \Longrightarrow \pi y^2 = \frac{2\pi R^2\left(1-\sqrt{1-\frac{x^2}{R^2}}\right)}{n/k}$$

This gives an equation for the base radius y (eq 9).

The function $r(z)$ is given by:

$$r(z) = (R+z)\sin\theta = (R+z)\frac{y}{R}$$

The height h is set by the requirement that the volume of all the stretching cones must be equal to the volume of species **B** polymer. The volume of one stretching cone is given by:

$$V_{1\mathrm{cone}} = \frac{1}{3}\pi(r(h))^2(h+R) - \frac{1}{3}\pi y^2 R = \frac{1}{3}\pi y^2\left(\frac{(R+h)^3}{R^2} - R\right)$$

Given that there are n half blocks of species **B** and there are N_B total species **B** monomers:

$$n\phi V_{1\mathrm{cone}} = \frac{4}{3}\pi b^3 N_B \Longrightarrow \frac{(R+h)^3}{R^2} - R = \frac{4b^3N_B}{n\phi y^2}$$

This gives an equation for the cone height h (eq 8).

Now to use the cone stretching equation (eq 13), $R_c(N')$ is needed. Given that each species **B** half block contains N_B/n monomers and assuming a linear increase of N' with z gives $z(N') = hnN'/N_B$. So:

$$R_c(N') = r(z(N')) = \left(R + \frac{hn}{N_B}N'\right)\frac{y}{R}$$

Hence by (eq 13) the stretching free energy (in units of kT) for each half block in species **B** is given by the integral:

$$F_S\left(\frac{1}{2}\mathbf{B}\ \mathrm{block}\right) = \frac{8b^4}{3\phi^2}\int_0^{N_B/n}(R_c(N'))^{-4}\,\mathrm{d}N'$$
$$= \frac{8b^4N_BR^4}{9hn\phi^2y^4}(R^{-3} - (R+h)^{-3})$$

This gives the total **B** stretching energy (eq 7).

Species A Stretching. The base radius of each cylinder is simply given by the base radius of the corresponding species **B** stretching cone y. If the height of each cylinder is H then by conservation of volume in species **A**:

$$n\phi V_{(1/2)\mathrm{block\ cylinder}} = \frac{4}{3}\pi b^3 N_\mathrm{A} \Longrightarrow H = \frac{4b^3N_\mathrm{A}}{3n\phi y^2}$$

Hence by the ideal stretching equation (eq 12), the stretching free energy in each cylinder is

$$F_S\left(\frac{1}{2}\mathrm{block\ cylinder}\right) = \frac{3H^2}{2N_Cb^2} = \frac{8b^4N_\mathrm{A}}{3n\phi^2y^4}$$

This gives the total **A** stretching energy (eq 10).

Relating *k* to *x*. The volume of one lens is

$$V_{\mathrm{Lens}} = 2(V_{\mathrm{cap+cone}} - V_{\mathrm{cone}})$$
$$= \frac{4}{3}\pi R^3\left(1-\sqrt{1-\frac{x^2}{R^2}}\left(1+\frac{x^2}{2R^2}\right)\right)$$

Given that species **A** consists of N_A monomers at a constant volume fraction ϕ:

$$k\phi V_{\mathrm{Lens}} = \frac{4}{3}\pi b^3 N_\mathrm{A} \Longrightarrow \frac{k\phi R^3}{b^3N_\mathrm{A}}$$
$$= \left(1-\sqrt{1-\frac{x^2}{R^2}}\left(1+\frac{x^2}{2R^2}\right)\right)^{-1}$$

Using the volume fraction equation (eq 4) to eliminate ϕ, an equation that relates the number of lenses k to the size of each lens x is obtained (eq 11).

■ ASSOCIATED CONTENT

Supporting Information. Text giving the solution to the propagator equation. This material is available free of charge via the Internet at http://pubs.acs.org/.

■ AUTHOR INFORMATION

Corresponding Author
*E-mail: rmholmes@stanford.edu.

■ ACKNOWLEDGMENT

The authors thank Matthew Pinson for useful discussions and his previous work.[10] The polymer conformation images were produced using the UCSF Chimera package from the Resource for Biocomputing, Visualization, and Informatics at the University of California, San Francisco (supported by NIH P41 RR001081).[17]

REFERENCES

(1) Dill, K.; Ozkan, S.; Shell, M.; Weikl, T. *Annu. Rev. Biophys.* **2008**, *37*, 289–316.
(2) Pack, D.; Hoffman, A.; Pun, S.; Stayton, P. *Nature Rev. Drug Discovery* **2005**, *4*, 581–593.
(3) Park, C.; Yoon, J.; Thomas, E. *Polymer* **2003**, *44*, 6725–6760.
(4) Matsen, M. *J. Phys.: Condens. Matter* **2002**, *14*, R21–R47.
(5) van den Oever, J.; Leermakers, F.; Fleer, G.; Ivanov, V.; Shusharina, N.; Khokhlov, A.; Khalatur, P. *Phys. Rev. E* **2002**, *65*, 041708.
(6) Khalatur, P.; Novikov, V.; Khokhlov, A. *Phys. Rev. E* **2003**, *67*, 051901.
(7) Vasilevskaya, V.; Khalatur, P.; Khokhlov, A. *Macromolecules* **2003**, *36*, 10103–10111.
(8) Williams, C.; Brochard, F.; Frisch, H. *Annu. Rev. Phys. Chem.* **1981**, *32*, 433–451.
(9) Parsons, D.; Williams, D. *Phys. Rev. Lett.* **2007**, *99*, 228302.
(10) Pinson, M.; Williams, D. 2010, Submitted for publication.
(11) Glotzer, S. C.; Solomon, M. J. *Nat. Mater.* **2007**, *6*, 557–562.
(12) van Blaaderen, A. *Nature* **2006**, *439*, 545–546.
(13) Kraft, D. J.; Hilhorst, J.; Heinen, M. A. P.; Hoogenraad, M. J.; Luigjes, B.; Kegel, W. K. *J. Phys. Chem. B* **2010**in press.
(14) Drolet, F.; Fredrickson, G. *Phys. Rev. Lett.* **1999**, *83*, 4317–4320.
(15) Fredrickson, G.; Ganesan, V.; Drolet, F. *Macromolecules* **2002**, *35*, 16–39.
(16) Zhang, Z.; Glotzer, S. *Nano Lett.* **2004**, *4*, 1407–1413.
(17) Pettersen, E.; Goddard, T.; Huang, C.; Couch, G.; Greenblatt, D.; Meng, E.; Ferrin, T. J. *Comput Chem.* **2004**, *25*, 1605–1612.
(18) Doi, M.; Edwards, S. F. *The Theory of Polymer Dynamics*; Oxford University Press: New York, 1986.
(19) Helfand, E. *J. Chem. Phys.* **1975**, *62*, 999–1005.
(20) de Gennes, P.-G. *Scaling Concepts in Polymer Physics*; Cornell University Press Ltd.: London, U.K., 1979.
(21) Holmes, R. Honours Thesis, The Australian National University, 2010.
(22) Helfand, E.; Tagami, Y. *J. Polym. Sci., Part B* **1971**, *9*, 741–746.